SST forcings and Sahel rainfall variability in simulations of the 20th and 21st centuries.

M. Biasutti [1] I. M. Held [2] A. Giannini [3] A. H. Sobel [4]

Corresponding author address: Michela Biasutti, Lamont-Doherty Earth Observatory of

Columbia University - Oceanography

61 Route 9W - PO Box 1000, Palisades, NY 10968-8000.

E-mail: biasutti@ldeo.columbia.edu

Short title:

[1]Lamont-Doherty Earth Observatory of Columbia University, Palisades, NY.

[2]Geophysical Fluid Dynamics Laboratory/ NOAA, Princeton, NJ.

[3]International Research Institute for Climate and Society, Palisades, NY.

[4]Columbia University, New York, NY.

ABSTRACT

The outlook for Sahel precipitation in coupled simulations of the 21st century is very uncertain, with different models disagreeing even on the sign of the anomalies. Such disagreement is especially surprising in light of the robust response of the same coupled models to the 20th century forcings.

We present a statistical analysis of the pre-industrial, 20th century and A1B scenario simulations performed by thirteen modeling groups in preparation for the IPCC fourth assessment report. We show that the relationship that links Sahel rainfall anomalies to tropical SST anomalies at interannual time scales in observations is reproduced by a vast majority of models in all simulations, independently of the change in the basic state as the world warms. Moreover, the same SST/Sahel relationship can be used to predict the simulated 20th century changes in Sahel rainfall from each model's simulation of changes in Indo-Pacific SST and Atlantic SST meridional gradient. Conversely, such a relationship does not explain the rainfall trend in the 21st century in a majority of models.

1. Introduction

During the second half of the 20th century Africa witnessed one of the most remarkable climate signals of the recent observational record in the pronounced negative trend in rainfall in the semi-arid Sahel, the southern edge of the Sahara desert, which culminated in the devastating drought of 1984 (e.g. Nicholson, 1980; Nicholson et al., 2000).

Given the large environmental and human impact of drought in this region, it is important to understand whether the drought of the 1970s and 1980s was a consequence of global warming and a harbinger of worse things to come, as many outside the scholarly community have already suggested (e.g., Gore, 2006), or whether the past drought was caused by other factors and the most recent upswing in rainfall (Nicholson et al., 2000) is the beginning of a steady recovery.

Our understanding of the Sahel drought has been growing thanks to many modeling studies that have employed both uncoupled and coupled general circulation models (GCMs). Recently, different atmospheric GCMs (Folland et al., 1986; Giannini et al., 2003; Tippett and Giannini, 2005; Lu and Delworth, 2005; Hoerling et al., 2006) forced with the historic timeseries of global sea surface temperature (SST), have been able to reproduce the 20th century Sahel pluvials and droughts, thus demonstrating that oceanic forcing has been the dominant driver of rainfall variability in this region. It appears that land surface and vegetation processes and perhaps dust feedbacks may amplify rainfall anomalies, but do not pace them (e.g., Zeng et al., 1999; Giannini et al., 2003; Rosenfeld et al., 2001)

Other modeling studies have tackled the question of whether one should attribute the 20th century Sahel droughts to internal climate variability or to anthropogenic emissions of greenhouse gases and aerosols. Rotstayn and Lohmann (2002) and Hoerling et al. (2006), following Folland et al. (1986) and others, have both emphasized the role

of the differential warming of the northern and southern hemispheres in determining the meridional location of the Atlantic ITCZ and the reach of the west African monsoon. Yet the former study argued for the role of anthropogenic aerosol in forcing Sahel drought, while the latter argued for natural variability. Giannini et al. (2003, 2005) and Bader and Latif (2003) have emphasized the warming of the tropical oceans, especially the Indian Ocean, as a possible cause of drying of the Sahel. Such a warming has been linked by Stott et al. (2000) and Knutson et al. (1999), among others, to anthropogenic greenhouse gases.

Biasutti and Giannini (2006) took advantage of the vast dataset produced by the international modeling community in preparation for the Intergovernmental Panel on Climate Change (IPCC) fourth assessment report and looked at Sahel rainfall variations in 19 different coupled GCMs. The vast majority of models (16 out of 19) simulate a significantly drier Sahel at the end of the 20th century with respect to the pre-industrial times. At least 30% of the observed long term drought was estimated to be externally—and most likely anthropogenically—forced. They concluded that, while the role of internal climate variability was predominant for the sharp 1950s-1980s decline in Sahel rainfall, anthropogenic influences have been substantial, giving reasons to worry about the future.

In simulations in which greenhouse gases are the only or dominant forcing, the agreement seen in the late 20th century response breaks down (Held et al., 2005; Biasutti and Giannini, 2006; Cook and Vizy, 2006; Lau et al., 2006). The fact that the 20th century drying does not continue in the 21st century in a majority of models would suggest that aerosols, and not greenhouse gases, have forced drought on the Sahel in the 20th century.

Biasutti and Giannini (2006) attribute the cross-model consensus in the 20th century integrations to the fact that models respond in a consistent fashion to the

cross-equatorial gradient of SST forced by reflective aerosols and Hoerling et al. (2006) point to the reversal in the Atlantic SST gradient as the global warming signal intensifies and aerosols go away as the cause of a predicted recovery in Sahel rainfall. Yet, Held et al. (2005) find that the coupled models of the Geophysical Fluid Dynamics Laboratory (GFDL) respond to increasing greenhouse gases with a very robust drying in the Sahel, even in the presence of a reversal of the Atlantic gradient. Moreover, simulations with uncoupled atmospheric models do indicate a drying of the Sahel in response to either a uniform warming or a warming of the Indian ocean (Held et al., 2005; Bader and Latif, 2003), which indicates that drying is a plausible response to increased greenhouse gases concentrations. Thus, as pointed out by several studies (Held et al., 2005; Cook and Vizy, 2006; Lau et al., 2006; Biasutti and Giannini, 2006), the outlook for rainfall in the Sahel is very uncertain: we do not know whether we should expect positive or negative rainfall anomalies in the Sahel under global warming.

The aim of this paper is to offer some insight on how such disparate predictions come about in different models. One possibility is that different models have different sensitivities to local and remote SST forcings of rainfall over the Sahel. For example, a warmer north Atlantic ocean could enhance the southerly flow and hence the moisture flux into the Sahel and could lead to more rain. A warmer Indo-Pacific ocean could, in analogy to a warm ENSO event, lead to a dryer Sahel. If different models weigh these processes differently, their outlooks for Sahel rainfall will differ as well. Another possibility is that the models predict patterns of SST anomalies for the 21st century that are different enough to force different Sahel responses, even if the sensitivities in each model are quite similar. Moreover, other forcings besides SST can become more important in the future: for example, land surface temperatures are expected to rise faster than SSTs (e.g. Houghton et al., 1995; Sutton et al., 2007), leading to an enhanced land-sea contrast and, possibly, monsoon rainfall (Haarsma et al., 2005). Again, models

might differ in how strong a land-sea contrast they predict or in how sensitive they are to this mechanism.

We focus on the role of changing SST in forcing changes in Sahel rainfall. We analyze the pre-industrial control integrations, the 20th century integrations and the 21st century so-called A1B scenario integrations of 19 among the IPCC AR4 models. We estimate the sensitivity of Sahel rainfall to local and remote SST forcings by looking at the strength of the statistical relationship between the Sahel rainfall index and the relevant quantities; and we address the question of whether it is possible to predict the 21st century response of a model to tropical SST changes from knowledge of its behavior in the 20th century.

In Section 2 we describe the integrations in more detail, introduce the models and assess their overall performance in simulating Sahel rainfall variability. In Section 3 we report on the statistical relationship between Sahel rainfall and SST, as simulated by the models in the pre-industrial and 20th century integrations. In Section 4 we investigate whether the relationships that have emerged at interannual timescales and in the forced changes of the 20th century are relevant for the 21st century trend. In Section 5 we offer our conclusions.

2. Datasets

Our dataset is extracted from the coupled model integrations assembled for the fourth assessment report of the Intergovernmental Panel on Climate Change. We have analyzed the 20th Century (hereafter XX), pre-industrial control (hereafter PI), and A1B scenario integrations (hereafter A1B) of nineteen coupled models. In the XX simulations, the coupled models are forced by the historic,varying concentrations of well-mixed greenhouse gases and sulfate aerosols, and—in some models—by other anthropogenic (e.g., black carbon particulate, or land use patterns) and natural

(solar output and volcanic aerosols) forcings. The PI controls have constant forcings, with CO_2 and aerosols concentrations held at the pre-industrial level. The A1B scenario assumes a growing world economy and technological advances, such that the concentration of CO_2 reaches 700ppmv in 2100 and stabilizes at that level, while aerosols concentration decreases. Table 1 provides a brief overview of the characteristics of the models. A full description of all models and integrations can be found at www-pcmdi.llnl.gov/ipcc/model_documentation/ipcc_model_documentation.php and references therein.

Our choice of models was dictated exclusively by the availability of the integrations when we recovered the data: we included all the available models, independently of the characteristics of their simulation over Africa. While it is likely that the 21st century simulation of Sahel rainfall can be compromised by a model's inability to reproduce the observed climatology or the observed relationship between Sahel rainfall and global SSTs, we do not know at this point what model characteristics are important in determining the 21st century response.

Figure 1 contrasts the annual cycle of rainfall averaged over 10°N-20°N across Africa in two observational datasets (CMAP, covering 1979-1999 (Xie and Arkin, 1996, 1997), and Hulme, covering 1900-1998 (Hulme, 1992)) and in the models (for each model we show the climatology in the PI, XX, and A1B integrations). There is a large spread across models in the amount of precipitation falling on the Sahel, with a tendency to underestimate it, sometimes dramatically (as for the IPSL model). All of the models at least capture the gross features of the mean seasonal cycle of Sahel rainfall, with maximum precipitation in the summer months, although some tend to simulate a faster increase of precipitation in the spring (for example the UKMO HADCM3), others a slower decline in the fall (e.g., CNRM CM3). The shape of the seasonal cycle is not appreciably or consistently changed across the PI, XX and A1B simulations, and thus

results in the rest of the paper are only shown for the northern monsoon season, defined as July, August, September (JAS).

In Figure 2 we explore the spatial characteristics of rainfall in the region. The contour lines show the mean position of summer rainfall over Africa and the Atlantic basin in observations and the coupled models. In observations (CMAP, Figure 2.xx), the maximum JAS precipitation extends over Africa from the equator to about 18N and is concentrated over the ocean in the Atlantic ITCZ, stretching from West Africa across the basin, at about 8N. Precipitation is more intense in the ITCZ than over the continent. The models show some fairly common biases. Over Africa, rain in many models does not extend far enough north; over the ocean, the ITCZ is often positioned too far south and widens over the Gulf of Guinea. (This bias is linked to most models' inability to develop a cold tongue in the Gulf of Guinea, see Davey et al., 2002)

Given that, in these models, the climatologies are far from perfect—and in particular that often the rainband stays shy of the Sahel—we provide a measure of how well the pattern of Sahel rainfall variability is captured by a single index defined on the basis of observations, as opposed to on the climatology of each model (say, by taking the Sahel to be straddling the 4mm/day isoline in each model). We define as Sahel index the JAS rainfall in the 10°N-20°N zonal band over Africa and calculate the correlation of global rainfall with this Sahel index in each PI integration (Figure 1, shading). In observations (Fig. 2.xx), correlations are—as expected—strong and positive in the region used to define the Sahel index, but are quite noisy elsewhere (this might in part be due to the shortness of the CMAP record). There is a signature of the dipole between the Sahel and the Gulf of Guinea, and of some positive correlation with rainfall at the northern edge of the ITCZ, although it is limited to a region near the coast. Overall, this Sahel index, which is based n observations, does capture the local rainfall variability in the coupled models, but the correlation patterns of Fig. 2 are affected by

the biases in the models' rainfall climatology. In some models the pattern is too narrow (e.g. Fig. 2.xv), in others too wide (e.g. Figs. 2.viii and 2.xviii), in others not zonal enough (e.g. Fig. 2.ii), in others weak enough to suggest little coherence across the Sahel (e.g. Figs 2.iii and 2.xvi). The correlations between the Sahel and oceanic precipitation also vary widely across models, with some models emphasizing the connection to the northern edge of the ITCZ (e.g. Fig. 2.xviii) and other emphasizing the dipole with Guinea (e.g. Fig. 2.xiii). In the remainder of this paper we will present results for the Sahel index as defined above, with the understanding that a few of the models do not accurately capture its mean magnitude, nor the associated spatial pattern of interannual variability.

3. Relationship between SST and Sahel rainfall in the PI and XX Integrations.

As many studies with atmospheric GCMs and prescribed SST have demonstrated, the Sahel droughts and pluvials recorded in the observational record were largely forced by SST. Thus, we begin this section investigating how the models reproduce the statistical relationship between Sahel rainfall and global SST. In this section we focus on the characterizes the natural variability and the 20th century trend.

Figure 3a displays a measure of the cross-model agreement in reproducing the linear correlation between the summer Sahel rainfall index and global surface air temperature at interannual-to-interdecadal timescales during pre-industrial times (for ocean regions, surface air temperature and SST are so tightly linked that we will use the two terms interchangeably). The figure is constructed in the following way. First, we calculate the correlation between the detrended Sahel rainfall and surface temperature time series for each of the 19 PI integrations (detrending should not be necessary, but some of the PI integrations experience climate drift); second, at every gridpoint we assign a value of +1

if the correlation is significant at the 95% level and positive, and -1 if it is significant and negative; third, we take the sum over all 19 models, and plot it as a percentage. An agreement of +80% would indicate that Sahel rainfall and temperature at that gridpoint are significantly, positively correlated in at least 80% of the PI integrations, with the remaining 20% of the models having either insignificant correlations, or as many positive as negative significant correlations.

There is a strong agreement across models on the fact that increased precipitation over the Sahel coexists with a locally cooler surface temperature, most likely because rain leads to cooling through increased surface evaporation. The positive Sahel correlation with surface temperature in the eastern Sahara and northern Arabian Peninsula is also very robust. Conversely, the relationship between Sahel rainfall and global SST is weaker, according to this metric. For example, there is only a 50% agreement that the Sahel index is significantly negatively correlated with SST in the tropical Pacific, and the agreement drops further in the eastern equatorial Pacific, where the ENSO signal, even in summer, should be strongest. When we repeat this calculation on a 5-year runnning mean, the agreement in the ENSO region becomes greater, suggesting some sensitivity to the details of the SST pattern, beyond the large scale warming or cooling (see also the discussion of Figure 4 below). The agreement on the anticorrelation with the south tropical Atlantic exceeds 60%, which is consistent with the strong relation seen in observations (Folland et al., 1986; Giannini et al., 2005); the correlation pattern in the north tropical Atlantic is weaker and somewhat noisy.

What emerges in Figure 3a is an overall inter-model agreement on the large scale pattern of correlation: the models indicate that at interannual-to-interdecadal time scales, a wet (dry) Sahel tends to be associated with cooler (warmer) tropics and a positive (negative) SST gradient across the tropical Atlantic. This pattern is quite similar to that seen in observations (see, for example, Figure 3 in Giannini et al., 2005).

One feature of the SST pattern that is more apparent here than in observations is the positive correlation of Sahel rainfall with mid-latitude surface temperature.

The relationship with SST that characterizes the interannual-to-interdecadal variability in Sahel rainfall is robust across different epochs, according to the IPCC models. Figure 3b (built as Figure 3a and showing the across-model agreement over significant correlation) shows that the pattern of correlation between the detrended time series of SST and Sahel rainfall in the XX simulations is remarkably similar to that in the PI case. The same result also holds for the global warming integrations A1B (see Figure 8 in the next section). We conclude that the interannual-to-interdecadal relationship between Sahel rainfall and surface temperature is left unchanged in its broader features as the the basic state changes under the effect of anthropogenic forcings.

To focus on the large scale pattern that has emerged in Figure 3, instead of looking at gridpoint-by-gridpoint agreement, and in order to consider each model individually, we now assess the relationship between Sahel rainfall and two indices of large-scale SST variability. Based on Figure 3 and the body of literature regarding the relationship between Sahel rainfall and SST, we choose as indices the mean Indo-Pacific SST (see for example Giannini et al., 2003, for the influence of ENSO and Indian Ocean SST on Sahel rainfall) and the North-South SST gradient in the tropical Atlantic. The studies that viewed the Sahel drought as part of a shift in the meridional position of the ITCZ have emphasized the role of either the local, Atlantic SST (e.g., Cook and Vizy, 2006) or a global, interhemispheric gradient (e.g., Folland et al., 1986); we choose to focus on the local SST gradient because we don't see in Figure 3 any evidence of inter-hemispheric antisymmetry in the pattern of correlation to SST: to the contrary, we see a high degree of symmetry in the two hemispheres, with negative correlation in the tropics and positive correlation poleward, only weakly disrupted in the north tropical Atlantic by a patch of positive correlations below 20°N and along the African coast.

To focus on the Sahel/SST relationship that emerges from natural variability, we analyze the PI integrations. We calculate the box average SST in the tropical Indo-Pacific (20°S-20°N; 50°E-90°W) and a bulk tropical Atlantic SST meridional gradient [north (7°N-30°N; 70°W-20°W) minus south (20°S-7°N; 40°W-5°E)] and calculate the correlation of these coarser indicators of patterns of SST anomalies with the Sahel index. Figure 4 shows that there is a much stronger model agreement according to this metric than in the case of gridpoint-by-gridpoint comparison. Correlations are more consistent and stronger when we filter out the fastest interannual variability with a 5-year running mean, so we discuss this case. Thirteen out of nineteen models have a significant (at the 95% level, shown in Figure 4 by the grey shading) negative correlation between the Sahel index and Indo-Pacific SST (two models show significant positive correlations), and fifteen models show significant positive correlations with the Atlantic north-south gradient (the rest of the models show insignificant, but still positive, correlations)[1].

The right panels of Figure 4 show the regression coefficients for a bi-variate linear model that uses the Indo-Pacifc SST and the Atlantic SST meridional gradient indices to "predict" variations in Sahel rainfall. According to this measure, although the relationship between the Sahel and the Atlantic is more robust, the relationship with the Indo-Pacific is more influential: the regression coefficients for the Indo-Pacific are about twice as large as those for the Atlantic.

Atmospheric general circulation models forced by historic SST can reproduce

---

[1]Correlations with single basins are somewhat less robust than with the 5-year running averaged Indo-Pacific and Atlantic gradient indices: correlations with the Pacific and South Atlantic indices resemble those to the Indo-Pacific and Atlantic gradient, respectively, but correlations with the North Atlantic change sign in different models, confirming the weaker relationship seen in Figure 3.

between 10% and 60% of the observed variance in Sahel rainfall (Hoerling et al., 2006). A poor-man's method to find out roughly how much of the Sahel rainfall variability can be captured by SST in the coupled integrations at hand is to use the simple bi-variate linear regression model constructed above and to then measure the likeness between the synthetic, or "predicted", Sahel and the original, simulated Sahel time series. Again, we focus on the 5-yr running means.

Figure 5a shows the correlation between the linearly predicted Sahel index and the original, simulated Sahel index in the integrations used to train the regression model (that is, the PI integrations). As expected, all models show positive correlations, and 13 show correlations better than 0.4. The fraction of variance in Sahel rainfall explained by SST is not large, compared to the estimates obtained from ensemble AGCM integrations with prescribed SST (Hoerling et al., 2006), but this was to be expected because we are using only one realization of a coupled integration, thus the variability linked to SST is a lesser fraction of the total variability. The spread among models is large: correlations range between about .7 (MRI) to virtually zero (CCSM3), an expected result given the range of Sahel/SST correlations shown in Figure 4.

Can we use the Sahel/SST relationship that we have derived from the natural variability in the PI integrations to interpret the behavior of Sahel rainfall in the presence of external forcings during the 20th and 21st centuries? Does the same relationship that explains variations in Sahel rainfall at interannual-to-interdecadal time scales work for explaining the Sahel trends in the 20th and 21st centuries? Here, we address these questions for the XX integrations; the case of the 21st century is explored in the next section.

Figure 5b shows the correlation between the XX simulated Sahel and the predicted Sahel (obtained from the XX SST indices, using the regression coefficients derived from the PI integrations) calculated either for the 5-yr running mean, detrended

timeseries (for which all variance is at timescales longer than interannual but shorter than centennial, and is dominated by natural variability, dots) or the 5-yr running mean timeseries (for which only the shortest timescales have been muted, and variance arises at all longer time scales, including the centennial trend, which is largely externally forced, squares). Only one realization of the XX simulations is used for each model. Our simple linear model—derived from the natural variability in pre-industrial times—has some predictive skill for the 20th century, whether we predict the full timeseries or only its shorter-term variability. Correlations between the original and the synthetic Sahel time series are positive in most cases (with the notable exception of the two NCAR and the MPI models), whether or not the centennial trend is included. This would seem to indicate that the trend in 20th century Sahel rainfall arises from the SST trends through the same mechanisms that shape the SST-forced interannual variability. The correlation between the "predicted" and simulated Sahel rainfall is in general somewhat better when we predict the full timeseries then when we predict only its short-term variability, which is consistent with the expectation that variability at shorter time scales would be affected by atmospheric internal variability more than would the trend.

A direct comparison (Figure 6) of the simulated Sahel 20th century trends with those linearly predicted from the XX SST confirms that the linear model captures the sign and order of magnitude of the simulated trends. In 11 out of 19 models the linear model produces a stronger drying trend than simulated; this could be just by chance, but the fact that the spurious increases of the negative trend are so much larger than any spurious decrease is suggestive of a tendency for the regression model to overestimates the drying trend.

As another test of the robustness of the SST/Sahel rainfall relationship, we perform a similar calculation, using the first half of the XX integrations to build a linear model for Sahel rainfall and validating the model by predicting Sahel rainfall changes in the

second half of the integrations. In this case we retain the trend in all timeseries, so that the forced component of the relationship can be captured by the linear model (to the extent that the forced signal is present in the early part of the 20th century and is not overwhelmed by natural variability at shorter timescales). The linear model shows some skill in a majority of models (Figure 7) but it is not as accurate as the model derived from the pre-industrial natural variability and it produces negative correlations between the predicted and simulated Sahel rainfall timeseries in 4 of the models during the validation period. It is possible that this inconsistency arises from the paucity of data on which the regression was built (about 50 or 70 years, compared to the 100 or 200 years for the PI simulations).

4. Relationship between SST and Sahel rainfall in the A1B Integrations.

The relationship with global SST that characterizes the natural variability of the Sahel is robust across epochs: the large scale pattern of correlation between the Sahel index and surface temperature that emerges from the A1B integrations at interannual-to-interdecadal timescales—when the trend is removed from the Sahel and temperature time-series—is indistinguishable from that of the pre-industrial and 20th century simulations (cf. Figure 8 to Figure 3 in the previous section). Things are very different when the trend is retained in the time series and determines the sign of the correlation (not shown). The agreement across models is extremely weak: in a majority of models the surface global warming is accompanied by a positive trend in Sahel rainfall, but in some models the warming is accompanied by drying and in others there is no significant correlation.

Figure 9 shows how, in each A1B simulation, the Sahel/SST relationship changes when the centennial trend is kept or removed. Specifically, Figure 9 shows the correlation

between the simulated and predicted 21st century Sahel for two linear regression models: the first is the one introduced in the previous section in Figs 4 and 5, the second is similar, but built on the entire XX runs (5-yr running means are applied, trend is retained). In both cases—whether the bi-variate regression model is built on the natural variability in the pre-industrial runs (Figure 9, left) or on the forced 20th century runs (Figure 9, right)—variations in SST capture only the interannual-to-interdecadal variations in Sahel rainfall (i.e. variations in the detrended time series, circles), but not the trend: in a majority of models the correlation between the simulated Sahel and the synthetic, SST-derived Sahel is negative when the trend is retained in the calculations (squares). To test whether the two predictors used for interannual variability were insufficient to capture the important pattern of SST anomalies in the forced 21st case, we also built a linear model using, besides the Indo-Pacifc, the north and south tropical Atlantic as independent predictors. Still, the AIB Sahel rainfall could not be captured in many of the models, regardless of whether the model was built from the PI or the XX integrations.

If one wanted to ascribe the disparate projections for 21st century Sahel rainfall to SST, one might consider a few possibilities: one is that the pathways of SST influence are the same across models and epochs, but different models produce different SST anomalies under global warming. Another possibility is that, although the SST anomalies are the same across models, each model weighs the influence of different ocean basins differently, so that a drying influence is dominant in one model, but not in others. A third possibility is that the linear response to SST change that was dominant in driving natural and forced anomalies in Sahel rainfall in the 20th century is not relevant anymore, with new influences arising either from non-linearities or from new patterns of SST anomalies. Finally, ascribing the disparate projections for 21st century Sahel rainfall to SST might not be possible: SST might cease to be the most important

driver for Sahel rainfall change in all the models, and new influences from some other factor in the climate system might become dominant.

The linear regression model presented in Figure 9 accounts for the first two possibilities: it takes into account both differences in trends and in the sensitivities. Thus, to the extent that linear thinking and our choice of SST indices are warranted, we already know that model discrepancies cannot be explained by SST. Nevertheless, we want to err on the side of completeness and show more analysis that explores discrepancies in trends and in sensitivities across models.

In Figure 10 we explore the possibility that different SST trends may cause different Sahel rainfall trends. We show the trend in Sahel rainfall, mean tropical Indo-Pacific SST, tropical Atlantic meridional SST gradient, and three more indices that describe in more detail the pattern of SST or atmospheric circulation changes in the Pacific: the difference in sea level pressure between gridpoints at Tahiti and Darwin, the difference in SST between the West and East Pacific, and the difference between the equatorial and subtropical SST in the Pacific. We have included these indices because they provide some insight on whether a model produces an El-Niño or La Niña like climate change pattern (in the first two cases) or simulates an enhanced equatorial response in the Pacific (a pattern that might better describe the structure of the global warming signal according to Liu et al., 2005). These indices capture details in the Indo-Pacifc anomalies not captured by the mean SST and might indicate changes in the circulation relevant for the Sahel. In all panels in Figure 10 the gray shading indicates the sign of the Sahel trend in each simulation.

As expected, the warming in the Indo-Pacific is a feature of all model simulations, and thus bears no direct relation to discrepancies in the sign of Sahel rainfall anomalies. Changes in the Atlantic gradient, instead, are much more model dependent, with different models producing anomalies of different signs, yet, there is no correspondence

between the anomalies in Atlantic gradient and those in Sahel rainfall. For example, the two MIROC models have differently signed anomalies in the gradient, but both produce strong positive anomalies in Sahel rainfall. Conversely, the two GFDL models dry the Sahel, but not (as already reported by Held et al., 2005) because of a negative trend in the Atlantic gradient. Discrepancies in the sign of the trend for the Pacific indices also fail to match those in Sahel rainfall trend, suggesting that even more refined indices of SST variations would fail to explain the 21st century changes in the Sahel in a consistent way across all models (this has been tested in regression models).

Finally, we present evidence that the sensitivity of Sahel rainfall to SST changes more consistently from one epoch to the next than from one model to another: Figure 11 shows the coefficients of three bi-variate linear regression models for Sahel rainfall that use the Indo-Pacific and Atlantic gradient indices as predictors and are based on the PI, XX, and A1B integrations.

We see that the relationship between the Sahel and the Atlantic gradient is quite consistent across epochs (and thus in the presence or absence of anthropogenic forcings). The relationship with the Indo-Pacific is stronger for many models, but it is more variable and is sensitive to the presence of the trend both in the 20th century (the coefficients maintain the same sign as in the PI integrations in most cases but their magnitude is, in general, much reduced) and especially in the 21st century (the regression coefficients become positive in a majority of models).

This suggests that the negative correlations between the simulated and linearly predicted Sahel in the A1B scenario shown in Figure 9, like those of Figure 7 for the latter part of the XX simulations, are a consequence of a changing relationship between the Sahel and the Indo-Pacific warming that becomes evident going from the pre-industrial to the 20th century and from the 20th to the 21st century.

5. Conclusions

The projection for Sahel rainfall changes in response to global warming is highly uncertain, with some coupled models predicting strong dry anomalies, others predicting strong wet anomalies, and most predicting more modest anomalies of both signs. This disagreement is even more puzzling when compared to the agreement of a vast majority of the IPCC models in reproducing a dry Sahel in the late 20th century, compared to the pre-industrial epoch.

Given that previous modeling studies have shown that global SST changes have paced the Sahel droughts and pluvials of the recent history, we have explored the statistical relationship between rainfall and global SST as it is simulated by the IPCC models in the pre-industrial (PI), 20th century (XX) and 21st century (A1B). The large scale features of the observed correlation between Sahel rainfall and global SST are reproduced by a majority of models in the context of their natural variability (that is, when we calculate correlations and regressions between detrended timeseries). Sahel rainfall is negatively correlated with the tropical Indo-Pacific SST and positively correlated with the tropical Atlantic meridional SST gradient.

We have used the PI integrations to construct a linear, bi-variate model that predicts Sahel rainfall variations from changes in Indo-Pacific SST and Atlantic SST gradient. This model has a fairly good skill in predicting interannual-interdecadal variability in Sahel rainfall in both the XX and A1B integrations. When it is used to predict centennial trends, the model is still accurate in the simulations of the 20th century, but fails during the 21st century in a majority of models.

From the above analysis we conclude the following: (i) at interannual time scales, the relationship linking Sahel rainfall to the global SST does not change in any significant or consistent way from the PI, to the XX, to the A1B cases; (ii) the forced component of Sahel rainfall variations during the 20th century can be explained by

the corresponding variations in the Indo-Pacific SST and the Atlantic SST meridional gradient; (iii) the centennial trend that characterizes Sahel rainfall changes in the A1B integration is not explained, for a majority of models, by the same linear link to SST that explained rainfall variations during pre-industrial times and the 20th century.

Basically, in the global warming scenario, the Indo-Pacific warms and there is little trend in the Atlantic gradient. By the mechanisms operating at interannual-to-interdecadal timescales, the Pacific warming would induce a drought in the Sahel, but most models simulate a wetting of the Sahel, hence the negative correlations between the predicted and simulated Sahel. Indeed, there is a very good correspondence between the models for which our "prediction" model fails and those that simulate a wetting of the Sahel in the 21st century.

It appears that the future, GHG-forced change in Sahel rainfall is controlled by different mechanisms, not captured by the simple linear relationship that has characterized the past. It may be that the pattern of forced SST anomalies simulated for the 21st century is different enough from the patterns seen at interannual time scales and in the forced response during the 20th century that different pathways of SST influence become dominant. It is possible that small scale features of the tropical SST anomalies not captured in our analysis (which is based on coarse indices) are essential to determine Sahel rainfall changes. Another possibility is that extratropical SST play an important role. Alternatively, it may be that the assumption of linearity fails or that SST is not the only player in a warmer world, and greenhouse gases or aerosols become capable of directly affecting Sahel rainfall. Our analysis cannot rule out any of these options.

Another important conclusion that arise from this analysis is that a faithful reproduction of the 20th century is not in itself assurance that any given model will be accurate in its prediction of the future. More specifically, the fact that two models both

dry the Sahel in the 20th century and do so through the same influence of SST anomalies, does not mean that they will behave similarly in a simulation of the future. Therefore, similarity with observations in a simulation of the 20th century climate appears to be a necessary but insufficient condition for a trustworthy prediction of the future.

REFERENCES

Bader, J. and M. Latif, 2003: The impact of decadal-scale Indian Ocean sea surface temperature anomalies on Sahelian rainfall and the North Atlantic Oscillation. *Geophys. Res. Lett.*, **30**(22), 2169.

Biasutti, M. and A. Giannini, 2006: Robust sahel drying in response to late 20th century forcings. *Geophys. Res. Lett.*, **33**, L11706.

Cook, K. and E. K. Vizy, 2006: Coupled model simulations of the west african monsoon system: 20th and 21st century simulations. *J. Climate*, **19**(15), 3681–3703, In press.

Davey, M., M. Huddleston, K. Sperber, P. Braconnot, F. Bryan, D. Chen, R. Colman, C. Cooper, U. Cubasch, P. Delecluse, D. DeWitt, L. Fairhead, G. Flato, C. Gordon, T. Hogan, M. Ji, M. Kimoto, A. Kitoh, T. Knutson, M. Latif, H. L. Treut, T. Li, S. Manabe, C. Mechoso, G. Meehl, S. Power, E. Roeckner, L. Terray, A. Vintzileos, R. Voss, B. Wang, W. Washington, I. Yoshikawa, J. Yu, S. Yukimoto and S. Zebiak, 2002: STOIC: a study of coupled model climatology and variability in tropical ocean regions. *Clim. Dyn.*, **18**, 403–420.

Folland, C. K., T. N. Palmer and D. Parker, 1986: Sahel rainfall and worldwide sea temperature . *Nature*, **320**, 602–687.

Giannini, A., R. Saravanan and P. Chang, 2003: Oceanic forcing of Sahel rainfall on interannual to interdecadal time scale. *Science*, **302**, 1027–1030.

Giannini, A., R. Saravanan and P. Chang, 2005: Dynamics of the African monsoon in the NSIPP1 atmospheric model. *Clim. Dyn.*, **25**(5), 517–535.

Gore, A., 2006: *An inconvenient truth*. Rodale Press.

Haarsma, R. J., F. M. Selten, S. L. Weber and M. Kliphuis, 2005: Sahel rainfall variability and response to greenhouse warming. *Geophys. Res. Lett.*, **32**, L17702.

Held, I. M., T. L. Delworth, J. Lu, K. L. Findell and T. R. Knutson, 2005: Simulation of Sahel drought in the 20th and 21st centuries. *Proc. Natl. Acad. Sci.*, **102**(50), 17891–17896.

Hoerling, M., J. Hurrell, J. Eischeid and A. Phillips, 2006: Detection and attribution of 20th century northern and southern African rainfall change. *J. Climate*, **19**(16), 3989–4008.

Houghton, J., L. Meira Filho, B. Callender, N. Harris, A. Kattenberg, K. Maskell and Eds., 1995: Climate change 1995: the science of climate change. p. 572pp., contribution of Working Group I to the Second Assessment of the Intergovernmental Panel on Climate Change. Cambridge University Press.

Hulme, M., 1992: A 1951-80 global land precipitation climatology for the evaluation of general circulation models. *Climate Dyn.*, **7**, 57–72.

Knutson, T. R., D. L. Delworth, K. W. Dixon and R. J. Stouffer, 1999: Model assessment of regional temperature trends (1949-1997). *J. Geophys. Res.*, **104**, 30,981–30,996.

Lau, K. M., S. S. P. Shen, K.-M. Kim, and H. Wang, 2006: A multimodel study of the twentieth-century simulations of sahel drought from the 1970s to 1990s. *J. Geophys. Res.*, **111**(D07111).

Liu, Z., S. Vavrus, F. He, N. Wen and Y. Zhong, 2005: Rethinking tropical ocean response to global warming: The enhanced equatorial warming. *J. Climate*, **18**, 4684–4700.

Lu, J. and T. Delworth, 2005: Oceanic forcing of the late 20th century Sahel drought. *Geophys. Res. Lett.*, **32**, L22706, doi:10.1029/2005GL023316.

Nicholson, S. E., 1980: The nature of rainfall fluctuations in subtropical West Africa. *Mon. Wea. Rev.*, **108**, 473–487.

Nicholson, S. E., B. Some and B. Kone, 2000: An analysis of recent rainfall conditions in West Africa, including the rainy seasons of the 1997 El Niño and the 1998 La Niña years. *J. Climate*, **13**, 2628–2640.

Rosenfeld, D., Y. Rudich and R. Lahav, 2001: Desert dust suppressing precipitation: A possible desertification feedback loop. *Proc. Natl. Acad. Sci.*, **98**(11), 5975–5980.

Rotstayn, L. D. and U. Lohmann, 2002: Tropical rainfall trends and the indirect aerosol effect. *J. Climate*, **15**, 2103–2116.

Stott, P. A., S. B. F. Tett, G. S. Jones, M. R. Allen, J. F. B. Mitchell and G. J. Jenkins, 2000: External control of 20th century temperature by natural and anthropogenic forcings. *Science*, **290**, 2133–21–36.

Sutton, R. T., B. Dong and J. M. Gregory, 2007: Land/sea warming ratio in response to climate change: Ipcc ar4 model results and comparison with observations,. *Geophys. Res. Lett.*, **34**(L02701).

Tippett, M. and A. Giannini, 2005: Potentially predictable components of African summer rainfall in a SST-forced GCM simulation. *J. Climate*, **19**(13), 3133–3144, In press.

Xie, P. and P. A. Arkin, 1996: Analyses of global monthly precipitation using gauge observations, satellite estimates, and numerical model predictions. *J. Climate*, **9**, 840–858.

Xie, P. and P. A. Arkin, 1997: Global precipitation: a 17-year monthly analysis based on gauge observations, satellite estimates, and numerical model outputs. *Bull. Amer. Meteor. Soc.*, **78**, 2539–2558.

Zeng, N., J. D. Neelin, K.-M. Lau and C. J. Tucker, 1999: Enhancement of interdecadal climate variability in the Sahel by vegetation interaction. *Science*, **286**, 1537–1540.
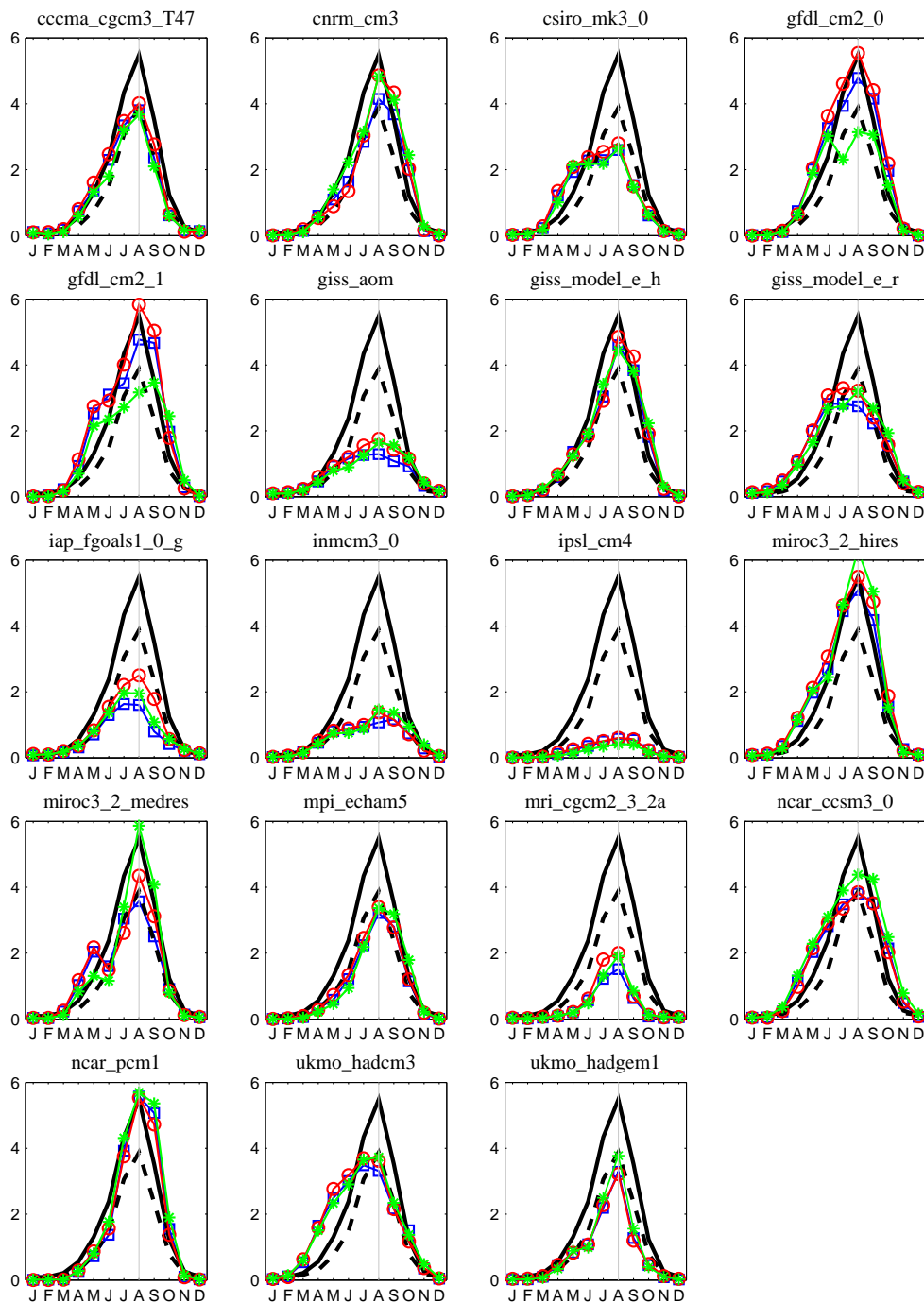
Figure Captions

Figure 1. Annual cycle of Sahel precipitation in observations (the solid black curve is the mean climatology in the Hulme dataset, the dashed black curve is CMAP) and in simulation of the pre-industrial epoch (PI, red circles), the 20th century (XX, blue squares), and the 21st century (A1B, green asterisks).
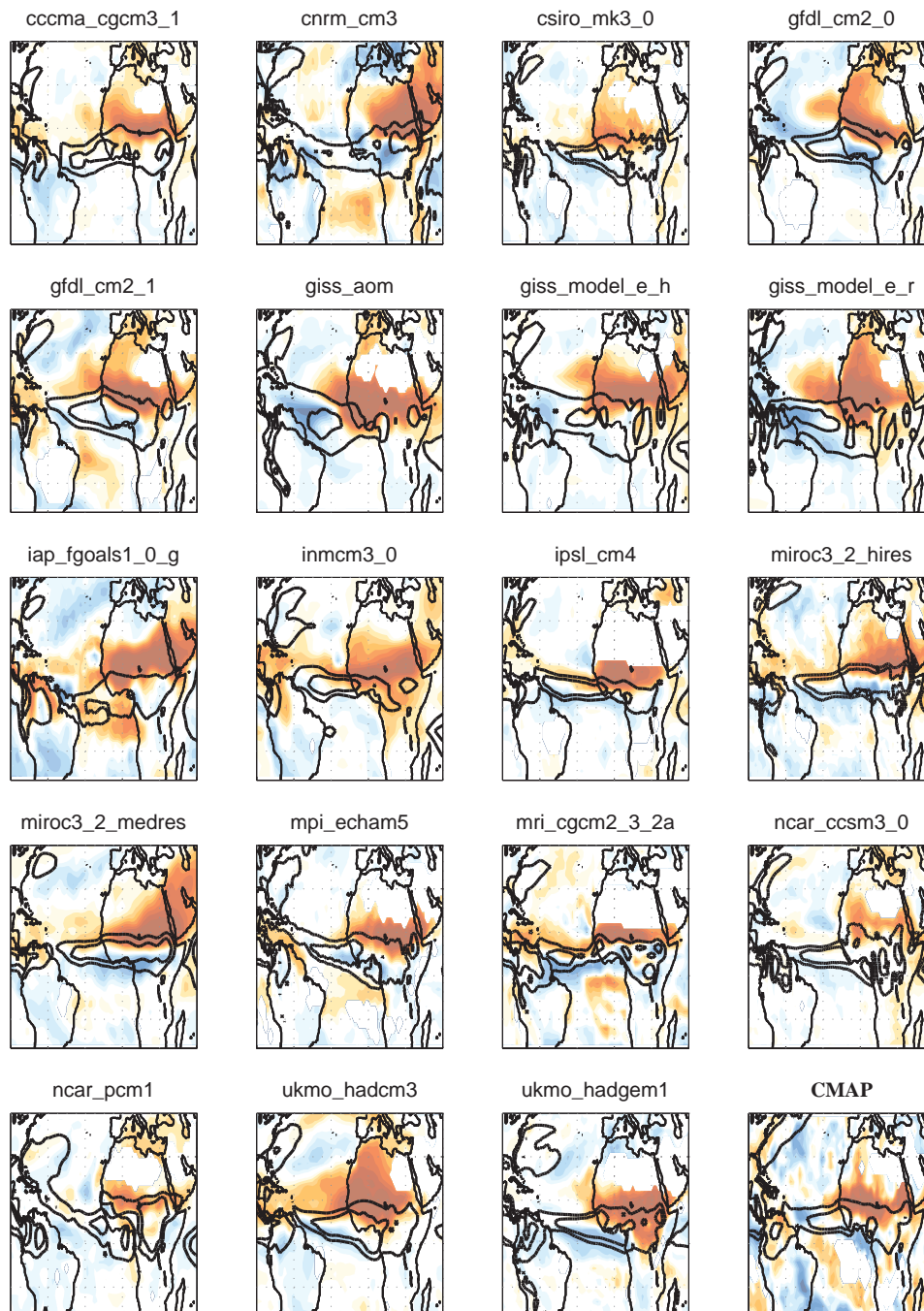
Figure 2. Contours: 4 and 8 mm/day contours of JAS precipitation. Shading: Correlation between the Sahel index and JAS rainfall. Warm colors indicate positive correlations, cold colors negative correlations, the shading interval is .08
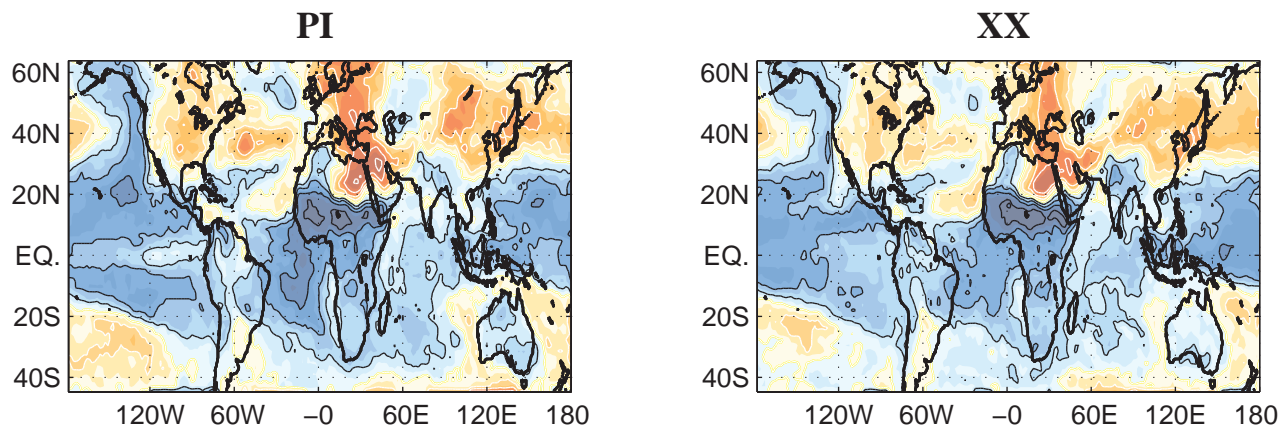
Figure 3. Percentage of models showing positive (dark grays / warm colors shading, white contours) or negative (light grays / cool colors shading, black contour) significant correlations between the Sahel index and surface temperature at each gridpoint. The left panel is for the PI detrended simulations, the right panel for the XX detrended simulations. The contour interval is 20%, the shading interval 40% (gray shading) or 10% (color shading). See text for further details.
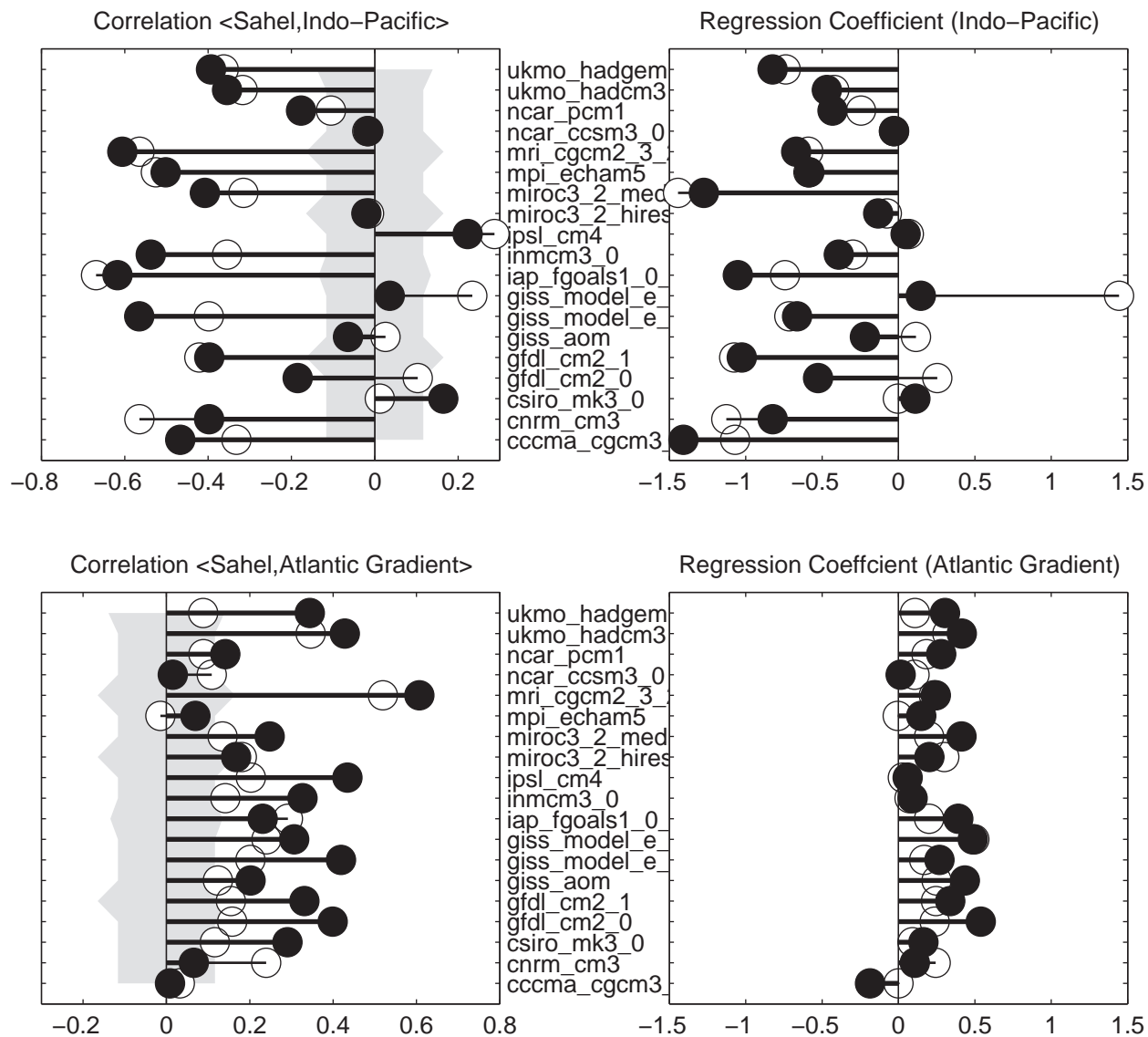
Figure 4. Pre-industrial correlations (left) and regression coefficients (right) between the Sahel index and (top) the area averaged Indo-Pacific SST and (bottom) the difference of north tropical Atlantic and south tropical Atlantic SST. Open circles are for timeseries that have been detrended; filled circles for detrended and 5-year running mean timeseries.
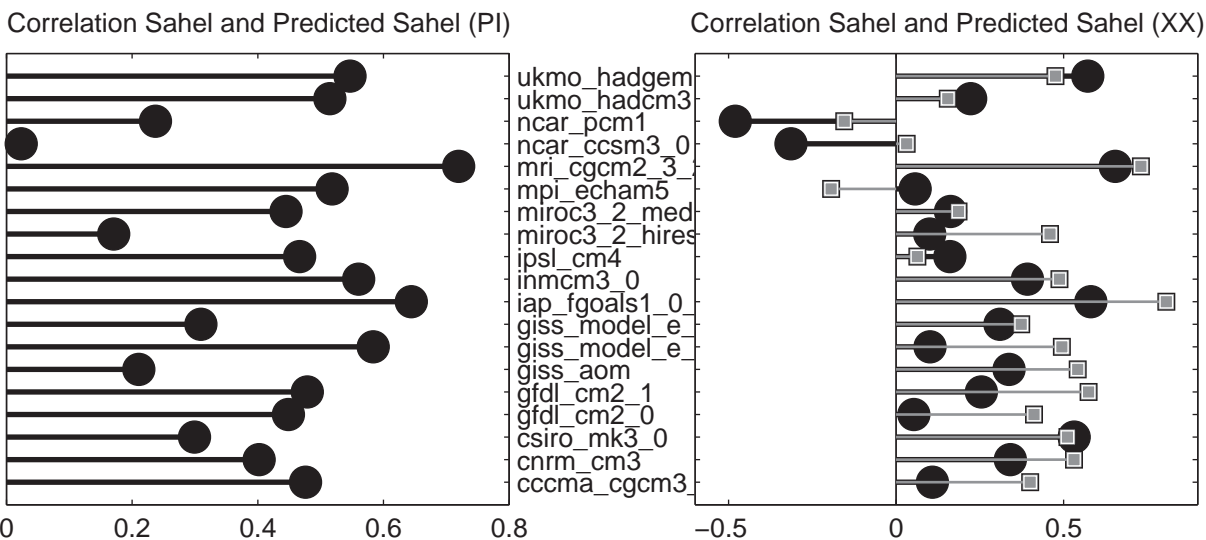
Figure 5. Correlations between simulated and linearly predicted Sahel index in the (left) PI and (right) XX integrations. The coefficients of the linear model come from the JAS, detrended, 5 year running mean time series of Sahel rainfall, Indo-Pacific SST and Atlantic SST gradient in the PI integrations. All timeseries have been subjected to a 5-yr running mean; dots refer to detrended timeseries, squares to timeseries retaining the trend.
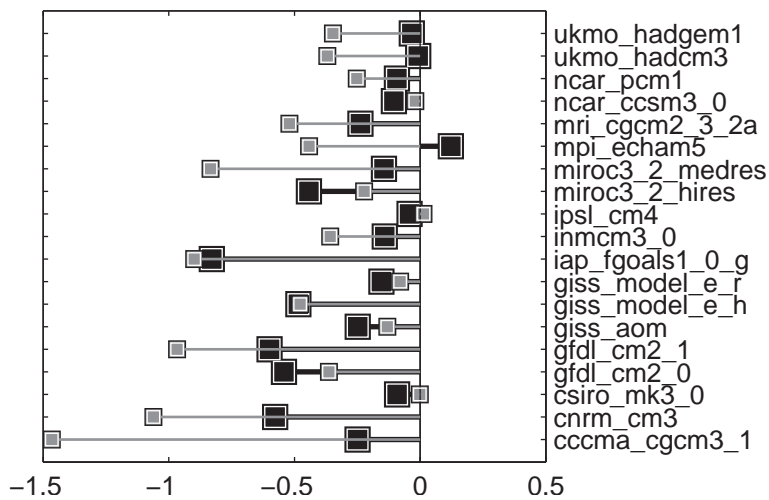
Figure 6. Linear trends in the simulated XX Sahel rainfall (large squares) and the "predicted" Sahel timeseries obtained by linear regression from the simulated XX SST (small squares). The linear regression model was trained on the detrended, 5-yr running means of the PI simulations. The trends are calculated over the length of the entire XX simulations, which might cover different periods for different models.
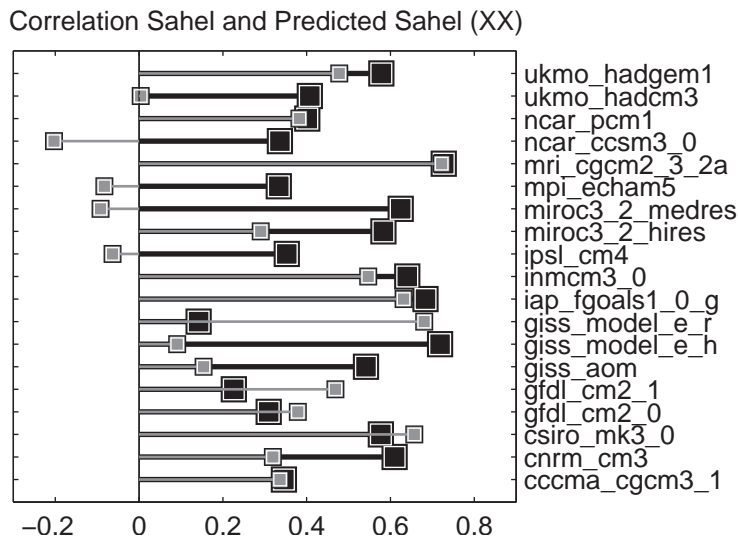
Correlation Sahel and Predicted Sahel (XX)

Figure 7. Correlations between simulated and linearly predicted Sahel index in the XX integrations. The coefficients of the linear model come from the JAS, 5 year running mean time series of Sahel rainfall, Indo-Pacific SST and Atlantic SST gradient in the first half of the XX integrations. Large, black squares refer to the first half of the XX simulations (training period), smaller gray squares to the second half of the XX simulations (validation period). Note that different XX simulations have somewhat different starting point, so that the training and validation periods are not the same for all models.
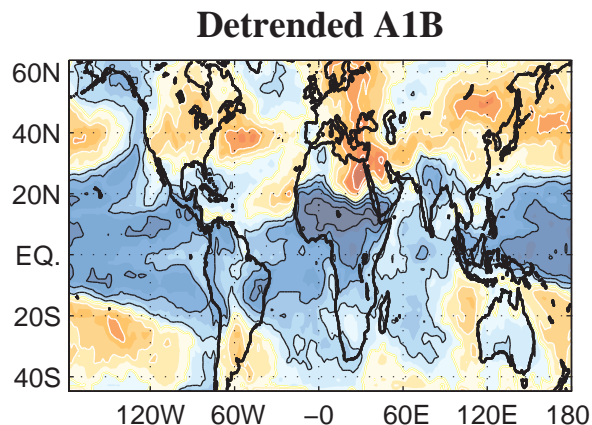
Detrended A1B

Figure 8. As in Figure 3 but for the A1B simulations.

A1B: Goodness of PI–based Linear Model   A1B: Goodness of XX–based Linear Model

ukmo_hadgem
ukmo_hadcm3
ncar_pcm1
ncar_ccsm3_0
mri_cgcm2_3_
mpi_echam5
miroc3_2_med
miroc3_2_hires
ipsl_cm4
inmcm3_0
iap_fgoals1_0
giss_model_e_
giss_model_e_
giss_aom
gfdl_cm2_1
gfdl_cm2_0
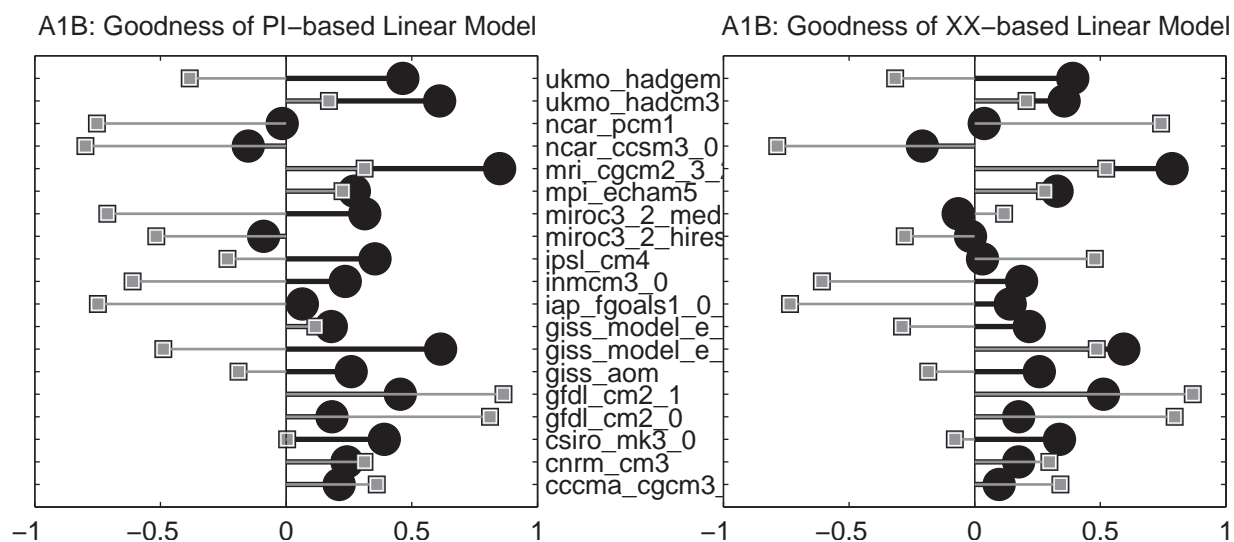csiro_mk3_0
cnrm_cm3
cccma_cgcm3

Figure 9. Correlations between simulated and linearly predicted Sahel index in the A1B integrations. The coefficients of the linear model come from the JAS, 5 year running mean time series of Sahel rainfall, Indo-Pacific SST and Atlantic SST gradient in the (left) detrended PI and (right) XX integrations. All A1B timeseries have been subjected to a 5-yr running mean; dots refer to A1B detrended timeseries, squares to A1B timeseries retaining the trend.
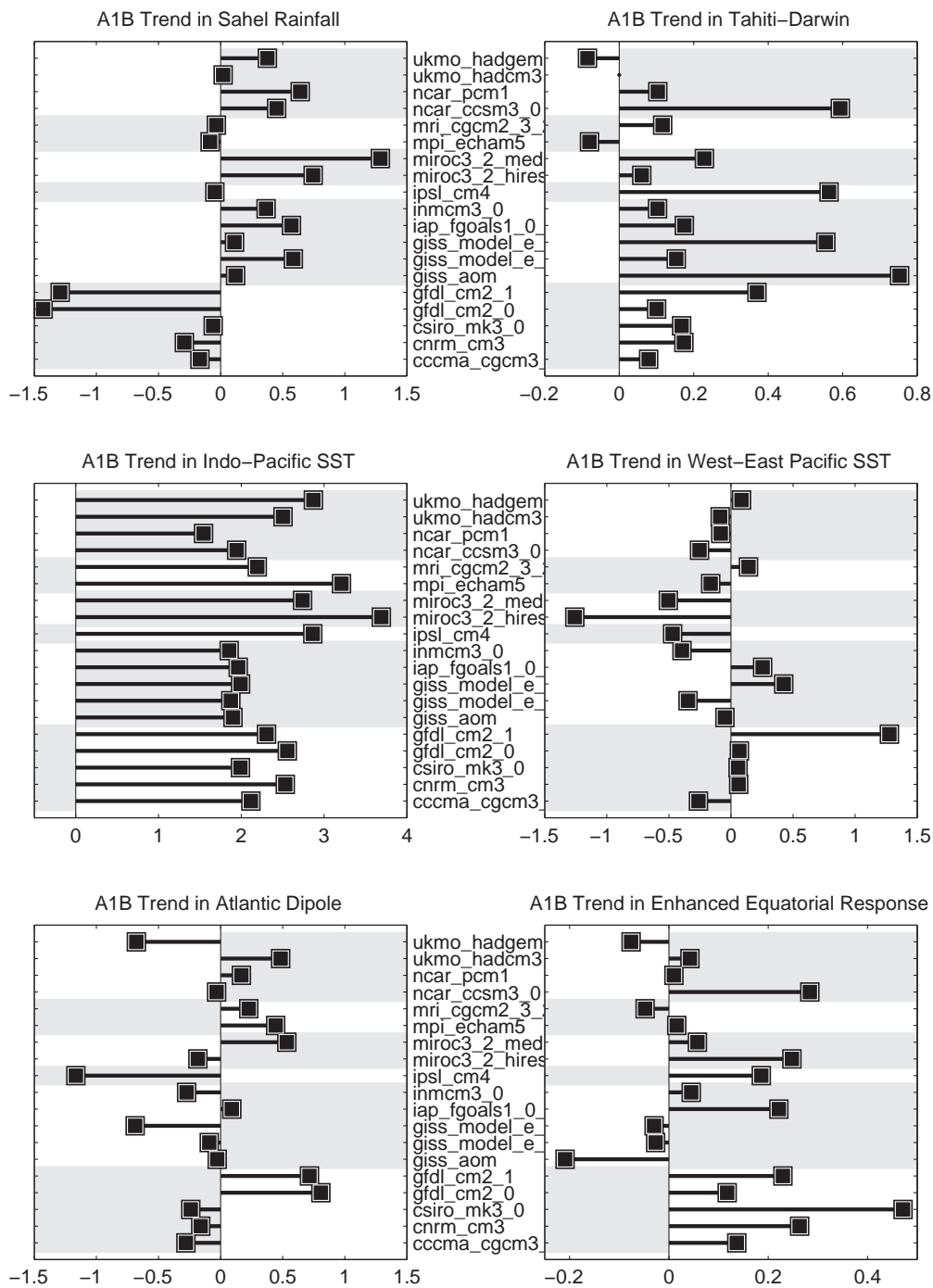
Figure 10. Linear trends over the years 2000-2100 in the A1B integrations in (top left) Sahel index, (middle left) Indo-Pacific SST, (bottom left) Atlantic SST meridional gradient, (top right) Tahiti-Darwin sea level pressure difference, (middle right) west equatorial Pacific - east equatorial Pacific SST difference, and (bottom right) the enhanced equatorial response index (Liu et al., 2005).
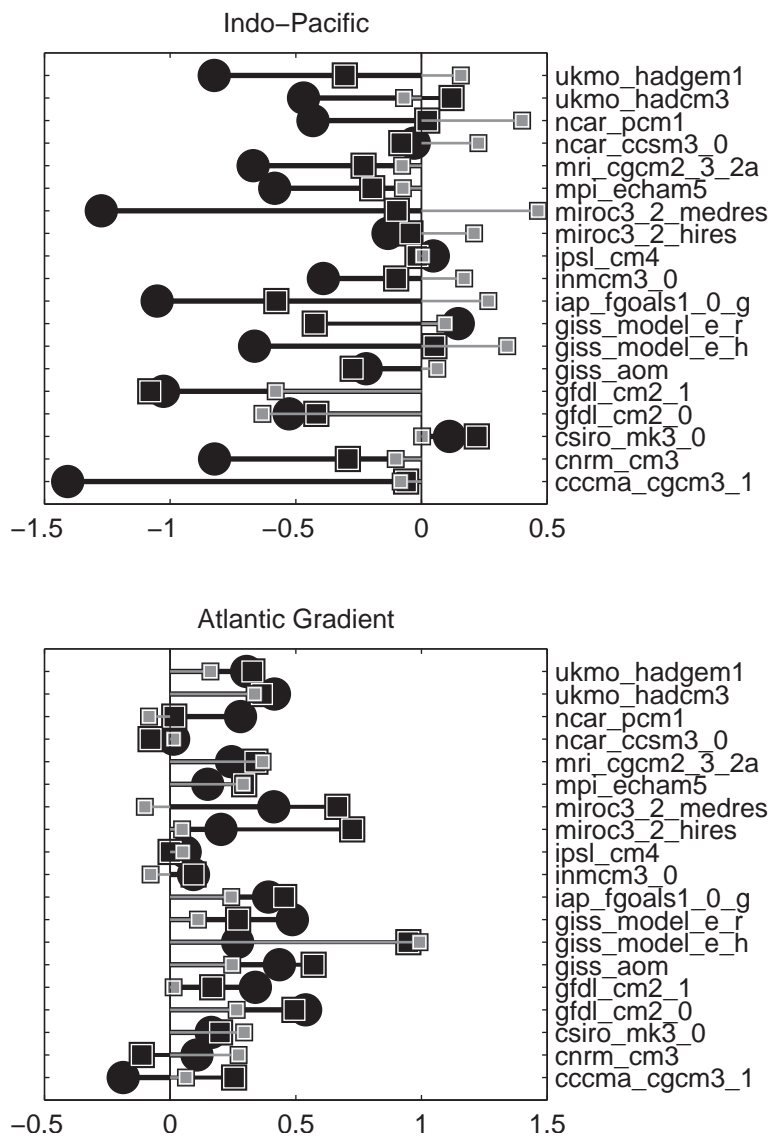
Figure 11. Bi-variate linear model regression coefficients between the Sahel index and (top) Indo-Pacific SST or (bottom) Atlantic SST meridional gradient. Dots are for the PI integrations, larger black squares are for XX and smaller gray squares are for A1B.

Tables

Table 1. Model name, Resolution of the atmospheric and oceanic component models (in degrees) and forcings used in the XX integrations, besides the increasing well-mixed greenhouse gases and the direct effect of sulfate aerosols: Natural forcings are solar output and volcanic emissions; Land refers to land use changes; OC is organic carbon, BC is black carbon, IE is the indirect effect of sulfate aerosols.

Model	Atmos.Resolution	OceanResolution	Additional 20th Century Forcings				
			Natural	Land	OC	BC	IE
ccma_cgcm3	3.75 x 3.71	1.85 x 1.85	N	N	N	N	N
cnrm_cm3	2.81 x 2.79	2 x 0.5	N	N	N	N	N
csiro_mk3_0	1.88 x 1.87	1.88 x 0.84	N	N	N	N	N
gfdl_cm2_0	2.5 x 2	1 x 1/3	Y	Y	Y	Y	N
gfdl_cm2_1	2.5 x 2	1 x 1/3	Y	Y	Y	Y	N
giss_aom	4 x 3	4 x 3	N	N	N	N	N
giss_model_e_h	5 x 4	2 x 2	Y	Y	Y	Y	Y
giss_model_e_r	5 x 4	5 x 4	Y	Y	Y	Y	Y
iap_fgoals1_0_g	2.81 x 3.05	1 x 1	N	N	N	N	N
inmcm3_0	5 x 4	2.5 x 2	Y	N	N	N	N
ipsl_cm4	3.75 x 2.54	2 x 1	N	N	N	N	N
miroc3_2_hires	1.13 x 1.12	0.28 x 0.19	Y	Y	Y	Y	Y
miroc3_2_medres	2.81 x 2.79	1.4 x 0.5	Y	Y	Y	Y	Y
mpi_echam5	1.88 x 1.87	1.5 x 1.5	N	N	N	N	Y
mri_cgcm2_3_2a	2.81 x 2.79	2.5 x 0.5	Y	N	N	N	N
ncar_cccsm3_0	1.41 x 1.40	1.13 x 0.27	Y	N	N	Y	N
ncar_pcm1	2.81 x 2.79	1.13 x 0.27	Y	N	N	N	N
ukmo_hadcm3	3.75 x 2.50	1.25 x 1.25	N	N	N	N	Y
ukmo_hadgem1	1.88 x 1.25	1 x 1/3	N	N	Y	Y	Y